Supporting Information

Gold nanoparticles integrated artificial nanochannels for label-free detection of peroxynitrite

Jing Wu, Xing Wang, Lei Ge, Rui Lv, Fan Zhang* and Zhihong Liu*

Hubei Collaborative Innovation Center for Advanced Organic Chemical Materials, Ministry of Education Key Laboratory for the Synthesis and Application of Organic Functional Molecules, College of Chemistry and Chemical Engineering, Hubei University, Wuhan 430062, PR China

E-mail: fanzhang@hubu.edu.cn; zhhliu@whu.edu.cn

1. Materials and reagent

Polyimide (PI) membranes (12 μm thick, 10^7 ion tracks per cm^2) were irradiated with heavy ion (Au) beams at UNILAC linear accelerator (GSI, Darmatadt, Germany). Sodium hypochlorite (NaClO, 13% available chlorine) was purchased from J&K Chemicals Co., Ltd. (Bejing, China). N-(4-Aminobutyl)-N-Ethylisoluminol (ABEI) was purchased from Tokyo Chemical Industry Co., Ltd. (TCI Shanghai, China). Chloroauric Acid ($HAuCl_4 \cdot 4H_2O$), polyvinylpyrrolidone (PVP), sodium borohydride ($NaBH_4$), potassium Iodide (KI), potassium chloride (KCl), hydrochloric acid (HCl), sulfuric acid(H_2SO_4, 98%), sodium nitrite ($NaNO_2$), hydrogen peroxide solution (H_2O_2, $\geqslant$ 30%), L-Ascorbic Acid (AA), L-Cysteine (Cys, 99%) were purchased from Sinopharm Chemical Reagent Shanghai Co. Ltd. (SCRC, China). Potassium superoxide (KO_2) was purchased from Alfa Aesar Chemical Co. Ltd; Sodium Sulfide (Na_2S) was purchased from Shanghai Titan Scientific Co. Ltd; Glutathione (GSH, Reduced) was purchased from Aladdin Biochemical Technology Co., Ltd.; Bovine serum and phosphate buffer saline solution (PBS) were obtained from Shanghai CHI Scientific Inc. All solutions were prepared in MilliQ water (18.2 MΩ).

2. Fabrication of conical nanochannels

The conical nanochannels were produced in a polyimide (PI) membrane using the well-known asymmetrical ion track etching technique. Before the chemical etching, each side of the polyimide membrane was irradiated by UV light (365 nm, 15W) for 1 hour. Then the membrane was sandwiched between two chambers of a conductivity cell at 50 ℃, one chamber was filled with etching solution (NaClO, pH $\approx$ 12.5), the other chamber was filled with stopping solution (1.0 M KI) that is able to neutralize the etchant as soon as the channel opens (Fig. S1). A voltage (DC = 1V) was applied to monitor the etching process. The etching process was stopped at a desired current value. Two chambers were added to a 1.0 M KI solution to neutralize the etchant, thus slowing down and finally stopping the etching process. After that, the membrane was immerged overnight in MilliQ water (18.2 MΩ) to remove residual salts. The diameter of the large opening (base) of the conical nanochannel was determined by scanning electron microscopy (SEM). The diameter d_{tip} of the small opening (tip) was evaluated using an electrochemical method in a parallel etching single nanochannel. For these studies, the PI membrane containing the single conical nanochannel was mounted in the conductivity cell and the transmembrane ionic current

was measured with 1 M KCl solution. The slope of the I-V curve is the ionic conductance (Fig. S2) and can be used to calculate the diameter of the tip opening by means of

$$d_{tip} = \frac{4LI}{\pi k(c)UD}$$

L is the length of the pore, which could be approximated to the thickness of the membrane after chemical etching; I is the measured ion current; U is the applied voltage; d_{tip} and D is the tip and the base diameter respectively; k(c) is the specific conductivity of the electrolyte. For 1 M KCl solution at 25 ℃, k(c) is 0.11173 Ω^{-1} cm^{-1}. In this work, the base diameter is about 520 nm and the tip diameter calculated to be ~ 16 nm.

3. Synthesis of ABEI@AuNPs

The AuNPs was synthesized according to the literature reported procedures. Primarily, $HAuCl_4 \cdot 4H_2O$ (24.4 mM, 1mL) was added to stirred deionized water (95 mL) in a 250 mL round-bottom flask with a condenser, heated to reflux for 10 min. Then, $NaBH_4$ (20 mM, 5mL) were gradually dropped into the $HAuCl_4 \cdot 4H_2O$ solution. Boiling the red solution was continued for 10 min. Subsequently, the solution was cooled to room temperature, and the solution was stirred for an additional 20 min. Subsequently, the obtained AuNPs (20 mL) was added with polyvinylpyrrolidone (0.002g) and ABEI for 8 hour, and color of the solution change from wine red to purple. The optimized concentration experiment of modification with ABEI was shown in Fig S4, and finally concentration of 1.0 mM ABEI was adopted for subsequent experiments.

4. Sample preparation

Peroxynitrite ($OONO^-$) stock solution was prepared by a reported method.[1] Primarily, to a stirred solution of $NaNO_2$ (0.6 M, 10 mL) in deionized water at 0 ℃was added H_2O_2 (0.7 M, 10 mL) and HCl (0.6 M, 10 mL) in turn, immediately followed by the rapid addition of NaOH (1.5 M, 20 mL). Afterwards, excess H_2O_2 was removed by passing the solution through a short column of MnO_2. The concentration of $ONOO^-$ was determined by UV–Vis analysis with the extinction coefficient at 302.0 nm (ε = 1670 M^{-1} cm^{-1}). Aliquots of the solution were stored at -20 °C for use.

Nitric oxide (NO) stock solution was prepared by adding dropwise the H_2SO_4 (3.6 M) into a stirred solution of $NaNO_2$. The generated gas was successively passing through a solution of

NaOH (2 M) and deionized H_2O to eliminate other NOx and purify the NO. Then, the purified NO was bubbled in electrolyte solution (50 mM KCl+5 mM PBS, pH 7.13) for 30 min at 25 °C to obtain the NO stock solution (1.8 mM).

O_2^{-}• stock solution was prepared by dissolving KO_2 (10 mM) in dry DMSO (5 mL) to make a superoxide radical anion solution. The concentration of the generated O_2^{-}• was calculated from the absorbance at 271 nm ($\varepsilon = 2006\ M^{-1}\ cm^{-1}$).

Other analytes (H_2O_2, ClO^-, NO_2^-, GSH, Cys, S^{2-} and AA) were conducted with the corresponding commercial reagent and diluted with electrolyte solution to get a desired concentration.

5. Ion current measurement

The label free system of gold nanoparticles integrated nanochannels was constructed by adding the solution of ABEI@AuNPs into the nanochannel testing system according to the literature report.[10] Ion currents were measured by a Keithley 6487 picoammeter (Keithley Instruments, Cleveland, OH). A pair of Ag/AgCl electrodes was placed in two sides of the conductivity cell to apply a transmembrane potential across the nanochannels, the anode faced the base of the nanochannels. Each current-voltage curve was measured by scanning the voltage from -2 V to 2V across the nanochannel membrane that was sandwiched between two chambers, and both chambers were filled with an electrolyte solution. All measurements were conducted at room temperature, and each test was repeated five times to obtain the average value at different voltages. The error bars were obtained from three repeated measurements.

6. Selectivity test.

Various reactive species including NO, O_2^{-}·, H_2O_2, ClO^-, NO_2^- , GSH, Cys, S^{2-}, AA and $ONOO^-$, were selected to check the selectivity of our method. In this test, each substance was added into the electrolyte solution containing ABEI@AuNPs with the final concentration of 1 μM. The mixed solutions were used as electrolytes in the current measurement. Other conditions were the same as the standard test procedure.

7. Serum sample analysis.

The fetal bovine serum sample was selected as real sample, and diluted by the buffered solution

(10 mM PBS, pH 7.13). The recovery experiment was verified in aliquots of 1% serum samples (3 mL) spiking into standard $ONOO^-$ with different concentrations at 0.22 μM, 0.28 μM and 0.38 μM, respectively. The current detection procedures were according to those above protocol.

8. EDS measurement.

The energy-dispersive X-ray spectrum (EDS) was taken by an Oxford instruments X-max 50 (JSM-IT 500). In order to illustrate whether the AuNPs adsorbed on the inner wall of nanochannels, the EDS of the nanochannels before and after treating with ABEI@AuNPs were tested (Fig.S10). The results showed no Au elements appeared, indicating the gold nanoparticles were not adsorbed on the inner channels.

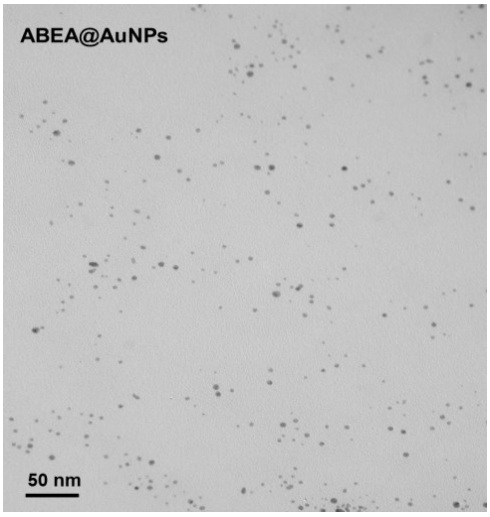

Fig. S1. TEM image of ABEA@AuNPs.

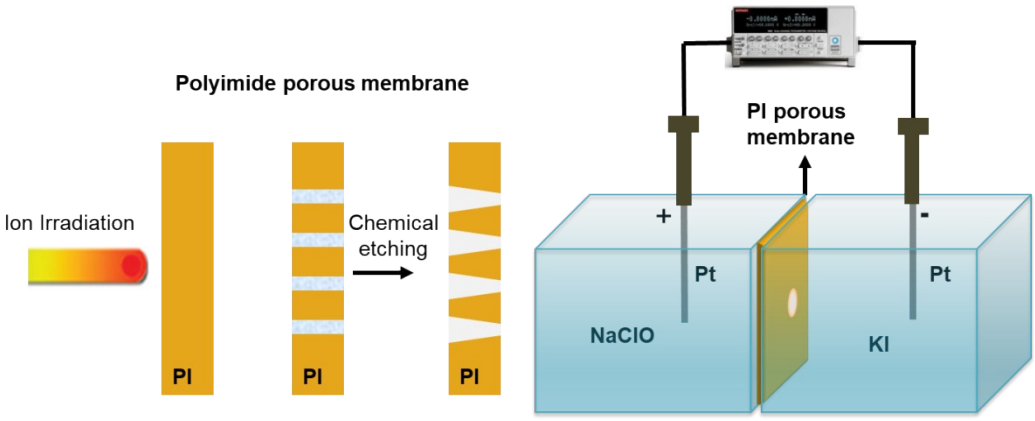

Fig. S2. Schematic image for etching conical nanochannels in a conductivity cell.

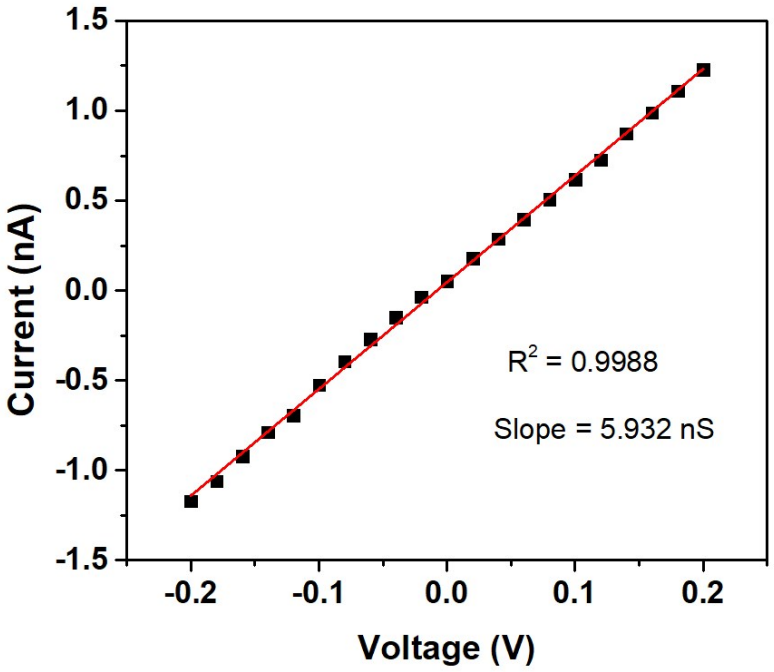

Fig. S3. I-V curves of the parallel etched membrane with single conical nanochannel in 1M KCl.

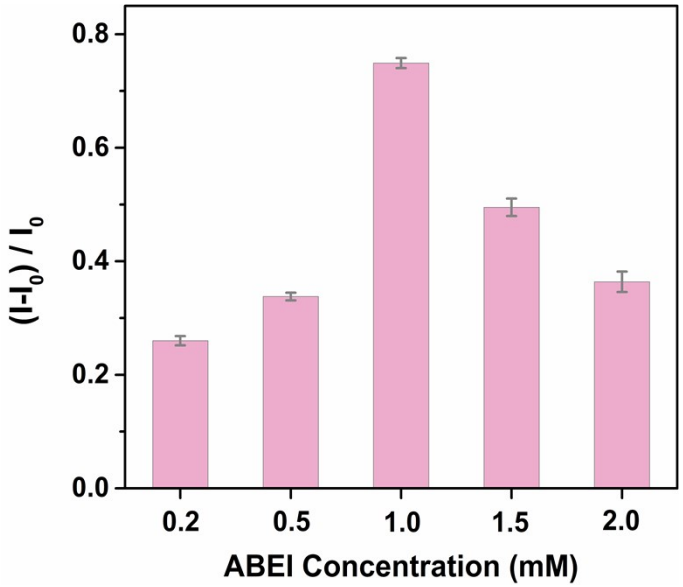

Fig. S4. Optimization of the experimental concentration of ABEI.

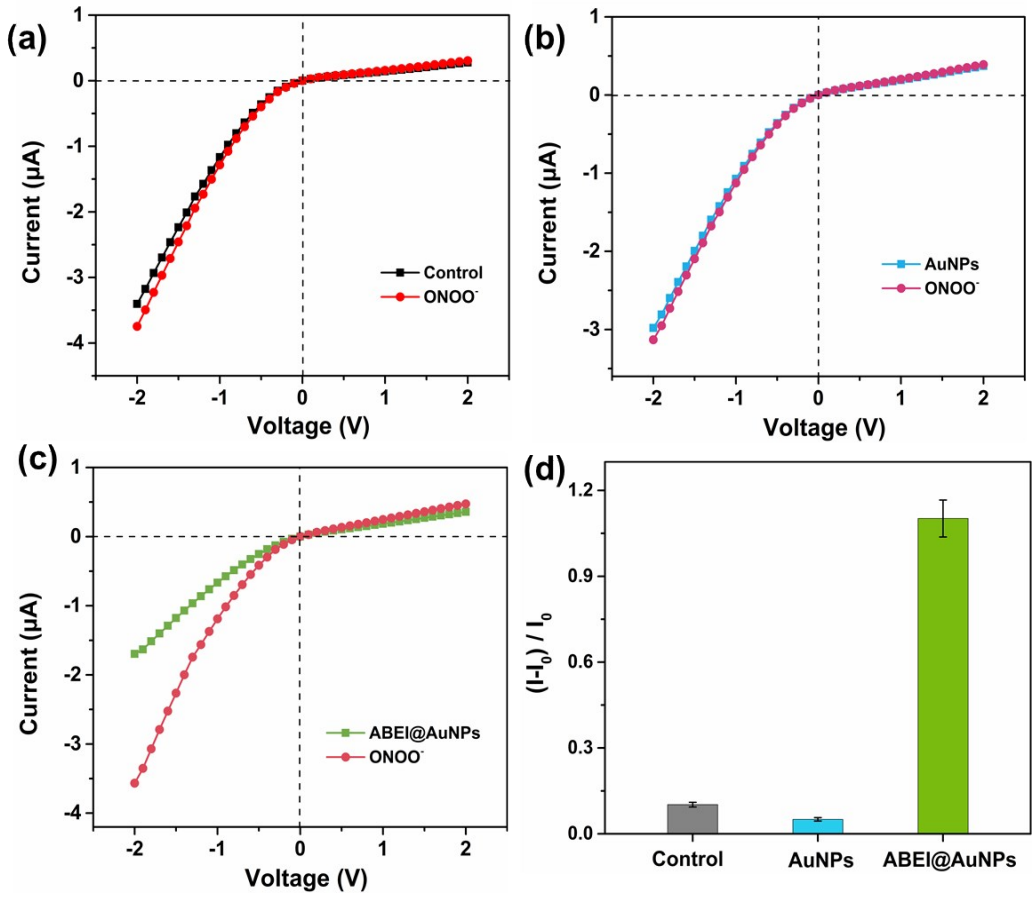

Fig. S5 I–V curves of the naked nanochannels (a), AuNPs integrated nanochannels (b) and ABEI@AuNPs integrated nanochannels (c) in the presence of 1 μM $OONO^-$, respectively. The current recorded in 0.05 M KCl buffer solution (5mM PBS, pH 7.13). (d) Histogram comparison of ionic current change ratios ($(I–I_0)/I_0$) at −2 V after responding to different reactive species.

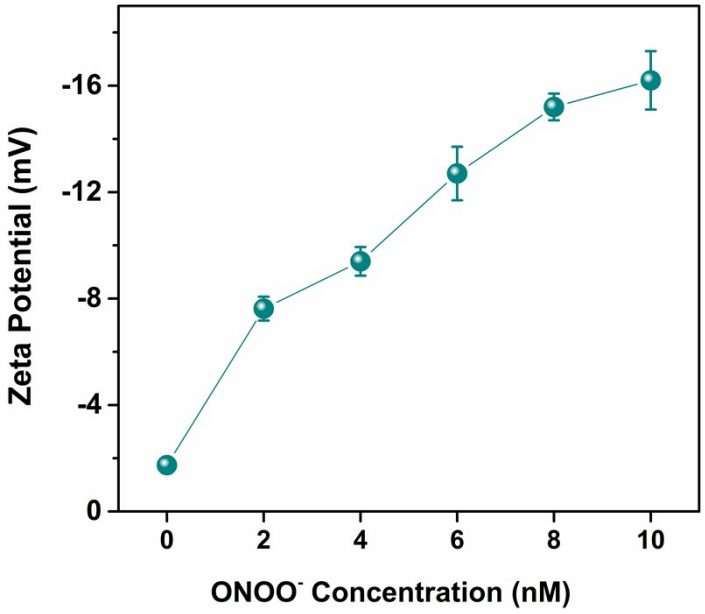

Fig. S6 Zeta potential of ABEI@AuNPs with addition of different concentrations of $ONOO^-$.

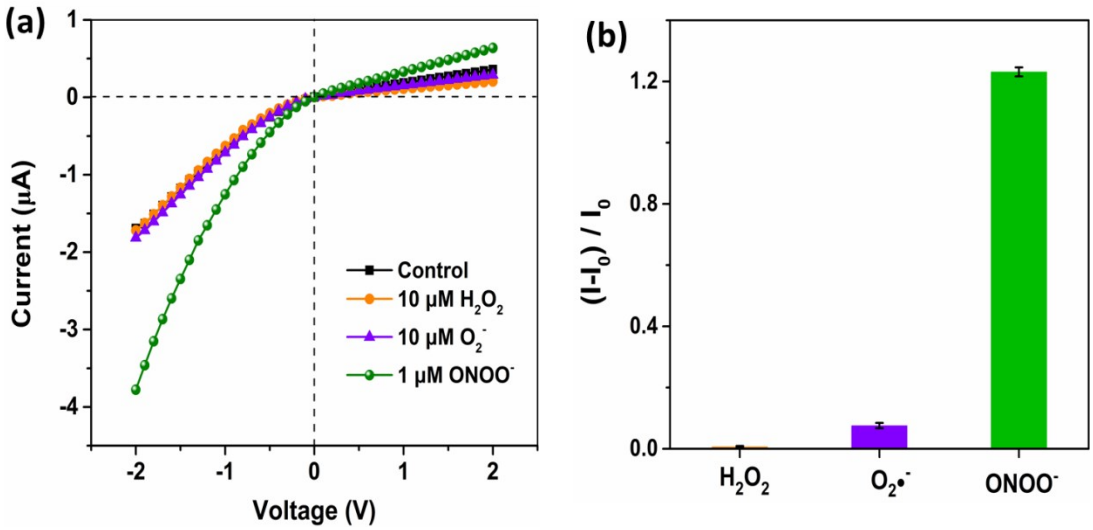

Fig. S7 I–V curves of the ABEI@AuNPs integrated nanochannels in the presence of 10 μM H_2O_2, 10 μM $O_2^{-\bullet}$ and 1 μM $OONO^-$, respectively. The current recorded in 0.05 M KCl buffer solution (5mM PBS, pH 7.13). (d) Histogram comparison of ionic current change ratios for different reactive species.

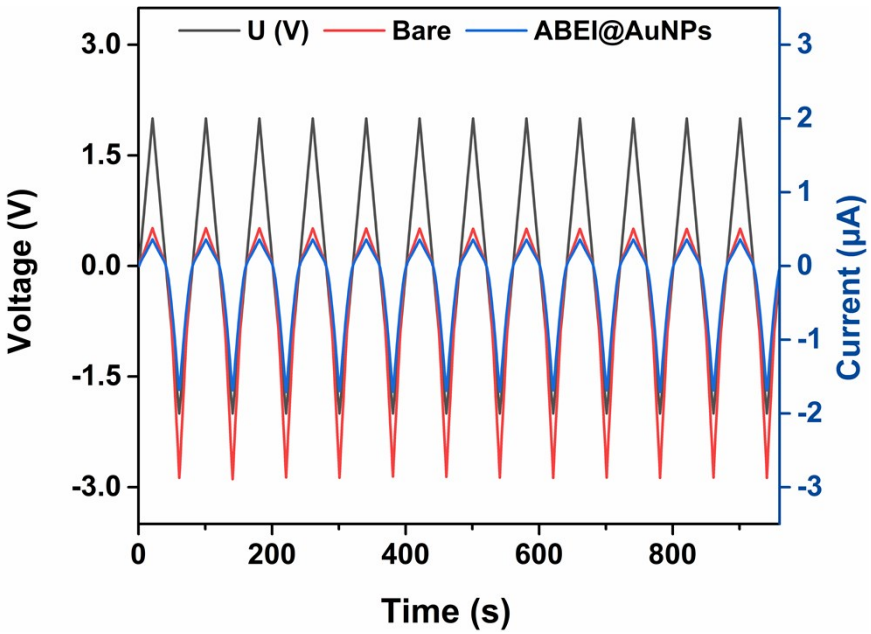

Fig. S8. Measurement cycles for the stability of the bare nanochannels before and after adding of ABEI@AuNPs obtained from the applied voltage and current signals in 0.05M KCl (pH = 7.13).

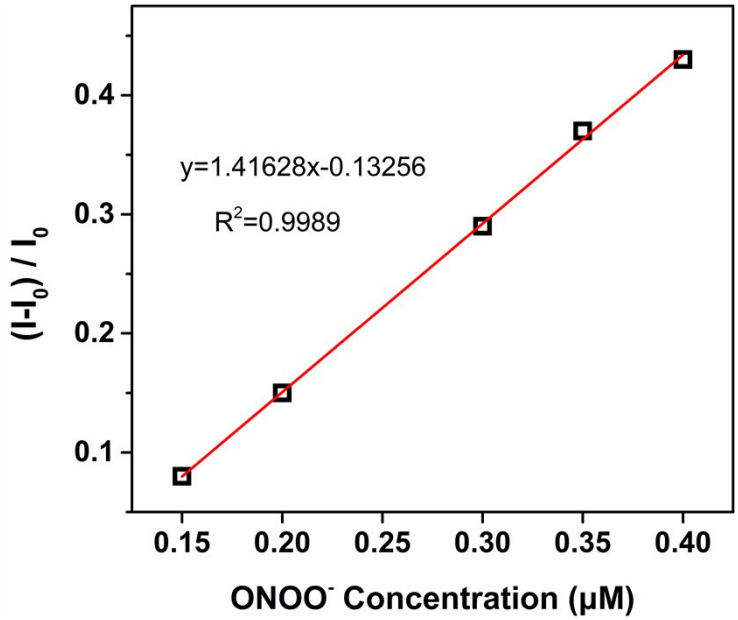

Fig. S9. Calibration curve of the $ONOO^-$ measured in bovine serum sample.

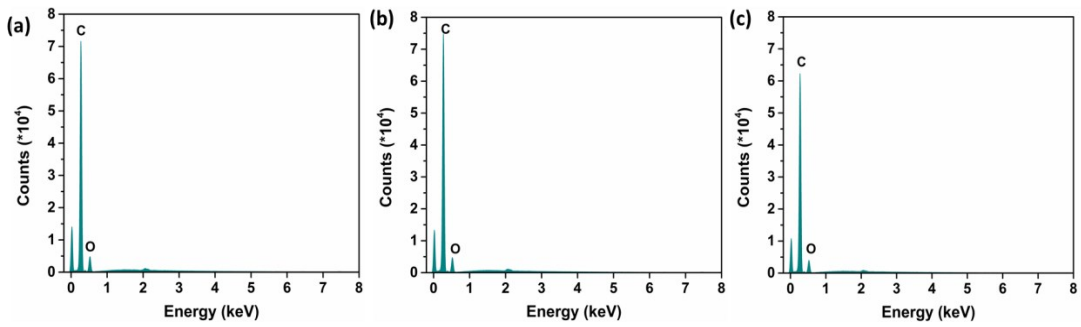

Fig. S10. EDS of (a) the bare nanochannel, (b) the nanochannels addition of ABEI@AuNPs and washed by water, (c) the (b) ABEI@AuNPs integrated nanochannels response with $ONOO^-$ and then washed by water.

Table S1. The XPS data of the unmodified AuNPs.

Name	Start BE	Peak BE	End BE	Height CPS	FWHM eV	Area (P) CPS.eV	Atomic %
Au4f	99.13	83.59	79.33	14656.65	1.44	43313.66	0.74
C1s	298.13	284.8	279.33	104297.16	1.76	223564.99	83.38
O1s	539.43	531.79	525.33	41044.74	2.34	112695.24	15.88

Table S2. The XPS data of the ABEI@AuNPs

Name	Start BE	Peak BE	End BE	Height CPS	FWHM eV	Area (P) CPS.eV	Atomic %
Au4f	99.43	83.75	79.63	15083.76	1.25	39623.33	0.63
C1s	298.53	284.8	279.73	112462.02	1.7	231393.87	80.79
O1s	540.33	531.7	525.63	41443.08	2.31	111262.16	14.68
N1s	410.43	399.81	392.63	7057.93	1.98	18055.12	3.9

Table S3. The XPS data of the ABEI @AuNPs after interaction with $ONOO^-$

Name	Start BE	Peak BE	End BE	Height CPS	FWHM eV	Area (P) CPS.eV	Atomic %
Au4f	96.51	83.48	79.61	502.53	1.26	2653.66	0.05
C1s	298.41	284.79	279.61	40275.29	1.68	91328.35	37.53
O1s	545.41	532.21	525.61	148050.93	2.15	389676.01	60.5
N1s	405.41	399.46	392.61	3024.64	1.88	7537.8	1.92

Table S4. Comparison of different methods for ONOO- detection.

Method	Probe	Linear range	LOD	Refs
Fluorescence	Ratiometric fluorescence probe (ABAH-LW)	up to 10 μM	21.4 nM	2
	AIEgen fluorescent probe (QM-ONOO−)	0-15 μM	27.5 nM	3
	O-CDs	0.3-9 μM, 9-48 μM	0.06 μM	4
Plasmon resonance energy transfer (PRET)	Au@MSN-CHCN nanoprobes	0.1-50 μM	47 nM	5
Surface enhanced Raman scattering (SERS)	AuNPs/MMP/MBAPE	1-100 μM	0.22 μM	6
	AuNP/3-MPBAPE	0.5-100 μM	0.4 μM	7
	AuNP/DAPBAP	0-100 μM	0.90 μM	8
Electrochemical	Hemin–PEDOT /CFE	0-40 μM	200 nM	9
Nanochannels	ABEI@AuNPs	0.02-5 μM	13.3 nM	**This work**

References:

[1] Z. Wang, W. Wang, P. Wang, X. Song, Z. Mao and Z. Liu, *Anal. Chem.*, 2021, **93**, 3035-3041.

[2] L. Wu, Y. Wang, M. Webera, L. Liu, A. C. Sedgwick, S. D. Bull, C. Huang and T. D. James, *Chem. Commun.*, 2018, **54**, 9953-9956.

[3] X. Han, X. Yang, Y. Zhang, Z. Lia, W. Cao, D. Zhang and Y. Ye, *Sens. Actuators B Chem.*, 2020, **321**, 128510.

[4] Y. Meng, Y. Jiao, Y. Zhang, W. Lu, X. Wang, S. Shuang and C. Dong, *J. Hazard. Mater.*, 2021, **408**, 124422.

[5] J. Wang, X. Li, H. Chen and J. Xu, *Anal. Chem.*, 2020, **92**, 15647-15654.

[6] D. Li, H. Chen, Z. Gan, J. Sun, D. Guo and L. Qu, *Sens. Actuators B Chem.*, 2018, **277**, 8-13.

[7] H. Chen, D. Guo, Z. Gan, L. Jiang, S. Chang and D. Li, *Microchim. Acta*, 2019, **186**, 11.

[8] H. Chen, E. K. Fodjo, L. Jiang, S. Chang, J. Li, D. Zhan, H. Gu and D. Li, *ACS Sens.*, 2019, **4**, 3234-3239.

[9] S. Peteu, P. Peiris, E. Gebremichael and M. Bayachou, *Biosens. Bioelectron.*, 2010, **25**, 1914-1921.

[10] I. Boussouar, Q. Chen, X. Chen, Y. Zhang, F. Zhang, D. Tian, H. S. White and H. Li, *Anal. Chem.*, 2017, **89**, 1110-1116.